ICP-1122

ALTERNATIVE FUEL CYCLE TECHNOLOGY PROGRESS REPORT FOR APRIL 1 - JUNE 30, 1977

CYRIL M. SLANSKY B. C. MUSGRAVE
B. R. DICKEY K. L. ROHDE

July 1977

Allied Chemical
IDAHO CHEMICAL PROGRAMS
IDAHO NATIONAL ENGINEERING LABORATORY
ENERGY RESEARCH AND DEVELOPMENT ADMINISTRATION
IDAHO OPERATIONS OFFICE UNDER CONTRACT EY-76-C-07-1540

Printed in the United States of America
Available from
National Technical Information Service
U.S. Department of Commerce
5285 Port Royal Road
Springfield, Virginia 22161
Price: Printed Copy $4.00; Microfiche $3.00

ICP-1122

UC-78
LWR Technology
TID-4500, R65

ALTERNATIVE FUEL CYCLE TECHNOLOGY
PROGRESS REPORT FOR APRIL 1 - JUNE 30, 1977

Cyril M. Slansky, Editor

Work performed under the direction of:

B. C. Musgrave, Manager
Technical Division

B. R. Dickey, Assistant Manager
Technical Division

K. L. Rohde, Assistant Manager
Technical Division

Date Published - July 1977

ALLIED CHEMICAL CORPORATION
IDAHO CHEMICAL PROGRAMS - OPERATIONS OFFICE

Prepared for

ENERGY RESEARCH DEVELOPMENT ADMINISTRATION
IDAHO OPERATIONS OFFICE
UNDER CONTRACT EY-76-C-07-1540

ABSTRACT

Quarterly progress is reported on alternative fuel cycle technology studies for the Savannah River Laboratory. Off-gas studies are reported on the reaction between NO_x and NH_3 and on the adsorption of gaseous iodine on silver-exchanged mondenite. Waste management studies include the evaporation and corrosion behavior of simulated high-level liquid waste in a thermosiphon evaporator and engineering studies on a laboratory-size storage tank.

SUMMARY

LWR OFF-GAS TREATMENT

Work is continuing on a topical report of the NO_x-NH_3 reaction catalyzed by hydrogen mordenite.

IODINE-129 ADSORBENT AND STORAGE DEVELOPMENT

Recycle tests on a bed of silver-exchanged mordenite, in which airborne-elemental iodine is repeatedly loaded and stripped, are being conducted with simulated dissolver off-gas streams. Loadings of 187 mg I_2/g substrate are being obtained. About 79% of the Ag is being used. No decline in iodine loading in the first 5 recycles is apparent.

Iodine loadings of 400 mg iodine per gram lead-exchanged faujasite have been obtained downstream of the silver bed during regeneration. About 90% of the lead is being used. Iodine-loaded lead-exchanged faujasite has a low iodine-vapor pressure and iodine-water solubility which may be suitable for storage.

The final draft of a report entitled, "Airborne Elemental Iodine Capacities of Metal Zeolites and a Method for Recycling Silver Zeolite", has been prepared. A process-flow diagram for full-scale application of silver-exchanged mordenite recycle technology to iodine recovery from dissolver off-gas streams is presented.

WASTE MANAGEMENT

The small-scale thermosiphon evaporator was operated successfully both with nitric acid and simulated high-level liquid waste (HLLW) during this quarter. The heat transfer coefficient varied from 760 to 2080 $W/m \cdot K$(134 to 367 $BTU/hr \cdot ft^2 \cdot {}^\circ F$) depending on the vapor velocities which varied from 0.3 to 1.22 m/s (1 to 4 ft/s). Scale, which formed on the reboiler tube during evaporation of the HLLW solution, is being investigated. The Type 304L stainless steel reboiler tube specimen had a corrosion rate of 517 μm/yr on a weight loss basis and 536 μm/yr based on the measured change of the inside diameter of the tube.

The laboratory storage tank and auxillary equipment have been completed and tested with water. The cooling coil water flow is entirely in the laminar flow range. A Reynolds number of 1000 was obtained at a nominal flowrate of 2.8 g/s. Improvements are continuing to reduce the 20 percent heat loss from the tank; this loss is at least partly due to the loss of nitric acid and heat in the condenser.

CONTENTS

FIGURES

TABLES

INTRODUCTION

This quarterly report is one of a series reporting progress by Allied Chemical Corporation - Idaho Chemical Programs at INEL on the Alternative Fuel Cycle Technology national programs which are administered by Savannah River Operations, ERDA, and the Savannah River Laboratory. Previous quarterly reports were published as ERDA reports ICP-1101, ICP-1108, ICP-1110, and ICP-1116.

The studies are identified as:

Off-Gas Treatment:	F-ID-13-001
Waste Management:	F-ID-13-002
^{129}I Adsorbent and Storage Development:	F-ID-13-004

RESULTS

I. LWR OFF-GAS TREATMENT

(R. A. Brown, D. H. Munger, T. R. Thomas)

Work is continuing on a topical report of the NO_x-NH_3 reaction catalyzed by hydrogen mordenite.

Future Plans

The topical report will be completed and the program terminated by October 1977.

II. ^{129}I ADSORBENT AND STORAGE DEVELOPMENT

(J. T. Nichols, L. P. Murphy, B. A. Staples, T. R. Thomas)

Recycle tests on a bed of silver-exchanged mordenite, Zeolon 900 (AgZ), in which airborne-elemental iodine is repeatedly loaded and stripped, are being conducted with simulated dissolver off-gas (DOG) streams. The experimental conditions are given in Table 1.

The AgZ test bed has been recycled five times. About 35 g of iodine is used for each loading; greater than 99% of the iodine is stripped at each regeneration. The loading tests are stopped when the decontamination factor is between 10^4 and 10^5. The results, along with the distribution of iodine from the top to the bottom of the bed, are given in Table 2.

The data indicate that the first 5 cm is in the saturation zone and the remaining 10 cm is in the mass-transfer zone. The average loading in the saturation zone is 187 mg I_2/g AgZ. The maximum loading in AgZ for complete conversion of Ag to AgI is 237 mg I_2/g AgZ. About 79% of the Ag is being used. No decline in iodine loading in the first 5 recycles is apparent; variations in the loadings are probably due to experimental error. The test bed will be recycled at least 15 times to check for loss of iodine-loading capacity.

An airborne-iodine concentration about four times greater than anticipated in actual DOG streams was used to shorten testing time. The iodine stripping rate is about ten times faster than the anticipated loading rate. However, the data given here are based on the initial 90% of iodine removed. Tests are being run to determine the tailing profile and average stripping rate based on 99% removal.

Iodine loadings of 400 mg iodine per gram lead-exchanged faujasite (PbX) have been obtained on PbX beds downstream of the AgZ bed during regeneration. The maximum iodine loading in PbX for complete conversion of Pb to PbI_2 is 440 mg. About 90% of the lead is being used. The vapor pressure of iodine chemisorbed on PbX (PbIX) has been estimated. Samples of PbIX

TABLE 1

Conditions for Recycle Tests

Experimental Parameter	Iodine Loading	Iodine Stripping
Bed Diameter (cm)	5	5
Bed depth (cm)	15	15
Particle size (mesh)	10-20	10-20
Superficial face velocity (m/min)	15	15
Bed temperature (°C)	150	500
Inlet pressure (mm Hg°)	700	760
Carrier gas	air	hydrogen
Iodine concentration at 21°C and 1 atm (mg/m³)	1500*	7400
NO_2 concentration (%)	2	0
NO concentration (%)	2	0
Dew point (°C)	35	nil
Iodine flux to and from bed (mg/min-cm²)	1.5**	4.5

---

*Actual DOG concentration is anticipated to be about 380 mg I_2/m^3
**Actual DOG iodine flux would be about 0.4 mg/min·cm²

TABLE 2

Iodine Loading vs. Number of Recycles

Cycle	mgI_2/g AgZ in each 2.5 cm segment 1	2	3	4	5	6	Ave. Loading mgI_2/g AgZ
0*	179	174	164	132	60	7	119
1	182	170	161	127	71	10	120
2	212	201	178	147	76	13	138
3	192	192	180	150	70	5	131
4	194	189	179	145	67	8	130
5	191	180	176	147	80	10	131

---

*The AgZ was pretreated with H_2 at 500°C for the initial loading cycle.

beads were placed in a heated optical cell and the vapor pressure of $I_2(g)$ vs. temperature determined from the absorption intensity of the $I_2(g)$ visible spectrum. Extrapolation of the data to room temperature indicated iodine-vapor pressures of less than 10^{-8} atm for PbIX in air, nitrogen, and hydrogen blankets. Beds of PbIX tagged with ^{131}I were immersed in hexane at room temperature for 16 hours to check for physisorbed iodine. Iodine in the hexane supernate was not detected. Previous tests have indicated that the water solubility of PbIX is less than that of PbI_2. The PbIX produced during the regeneration of AgZ is a dry yellow solid with a low iodine-vapor pressure and iodine-water solubility. Its physical properties and high iodine loading may make it an acceptable material for storage.

The final draft of a topical report entitled, "Airborne Elemental Iodine Loading Capacities of Metal Zeolites and a Method for Recycling Silver Zeolite", has been prepared. The process-flow diagram, which was used in the report, for full-scale application of AgZ recycle technology to iodine recovery is shown in Figure 1. Tables 3, 4, and 5 present the operational characteristics of an LWR fuel reprocessing plant, the laboratory data, and the design criteria, respectively.

The AgZ primary bed was sized for a 30-day loading operation. During the adsorption of iodine, the bed would attain some saturation loading of H_2O, NO_x, HNO_3, and ^{85}Kr. We have assumed an upper limit of 51 kg of H_2O and 36 kg of NO_2 for 0.65 m^3 of AgZ. During the 48-hr purge cycle, an average of 1.8 kg/h$\cdot NO_x \cdot H_2O$ would be added to the 11.7 kg/h$\cdot NO_x \cdot H_2O$ already present in the DOG. The combined load would increase the NO_x-H_2O flow to the parallel AgZ primary bed (not shown in flow diagram) by about 13% over normal operation. The two parallel AgZ adsorbent trains permit continuous iodine recovery while one of the beds is being regenerated.

After the purge cycle, the AgZ bed is isolated from the DOG and opened to streams No. 6-11. The air in the bed is purged off with nitrogen and vented just before the nitrogen inlet. Hydrogen is added to the nitrogen until the regeneration gas consists of 100% H_2. The AgZ primary bed is brought up to temperature, and the iodine stripped as hydrogen iodide. Any chemisorbed bromine would also be removed as HBr but at a rate 100 times faster than iodine. The desorbed iodine and bromine are chemisorbed as some form of lead halide on the PbX. Residual water on the AgZ and the PbX beds would be partially removed by the condenser. The regeneration process is a closed loop in which the H_2 is recirculated. Although 9 kg H_2/h would be recycled, only 4 kg H_2/y would be required to transport the halides as HI and HBr to the PbX.

The transfer of iodine to the PbX would be discontinued when iodine is detected in stream No. 8. The self-contained cartridges in the PbX storage bed would be removed and placed in 0.2 cubic metre (55-gal) drums for storage. The PbX backup-bed cartridge would be repositioned at the top of the PbX storage-bed holder and new cartridges placed below it and in the backup-bed holder. This would provide a fresh backup bed for every new set of cartridges placed in the PbX storage-bed holder.

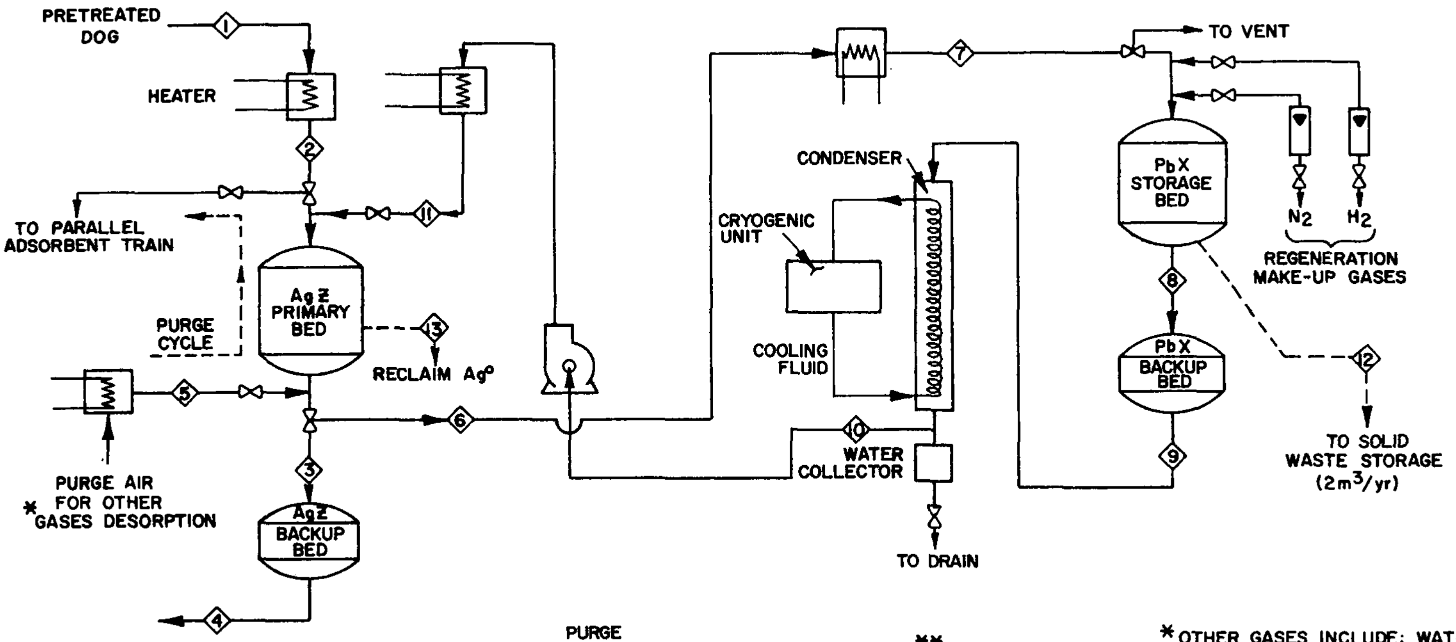

	LOADING CYCLE = 30 DAYS				PURGE CYCLE 2 DAYS	** REGENERATION CYCLE = 3 DAYS					
STREAM NO.	1	2	3	4	5	6	7	8	9	10	11
PRESSURE (atm)	1.0	1.0	0.8	0.75	1.1	0.94	0.94	0.87	0.85	0.85	1.0
TEMPERATURE (°C)	45	150	150	150	300	500	150	150	150	0	500
FLOW (m^3/h)	209	278	346	369	56	296	161	174	178	114	278
FLOW (kg/h)	233	233	233	233	38	9.6	9.6	9.6	9.6	9.6	9.6
NITROGEN	166	166	166	166	28	0	0	0	0	0	0
OXYGEN	51	51	51	51	9	0	0	0	0	0	0
OTHER GASES *	14.6	14.6	14.6	14.6	0.5	>0.6	>0.6	>0.6	>0.6	<0.6	<0.6
HYDROGEN	0	0	0	0	0	9	9	9	9	9	9
IODINE	7.1×10^{-2}	7.1×10^{-2}	7.1×10^{-4}	7.1×10^{-6}	0	0.26	0.26	2.6×10^{-3}	2.6×10^{-6}	2.6×10^{-6}	2.6×10^{-6}

* OTHER GASES INCLUDE: WATER VAPOR, NO_x, ARGON, AND KRYPTON AT 4.3, 7.4, 2.8 AND 0.09 kg/hr RESPECTIVELY.

** FLOWS FOR CLOSED LOOP. ABOUT 4 kg/yr H_2 NEEDED TO TRANSFER IODINE AS HI FROM AgZ TO PbX.

◇12 SPENT PbX TO WASTE STORAGE

◇13 LIFETIME OF AgZ UNKNOWN.

ACC-A-2622

Figure 1. Process Flow Diagram for the Recovery of Iodine From Dissolver Off-Gas

TABLE 3

Assumed Operational Characteristics
of an LWR Fuel Reprocessing Plant

1. Plant capacity	2000 tonne/y
2. Fuel burnup	28 700 MWd/tonne
3. Cooling period	1.5 y
4. Plant on-stream time	300 d/y
5. Air flow through dissolver at 0°C and 1 atm press	2.83 m^3/min
6. DOG pretreatment systems before iodine removal	H_2O/NO_x scrubber, de-entrainer, silica gel, and HEPA
7. NO_x conc. after pretreatment	≤2%
8. H_2O dew point after pretreatment	35°C
9. Volatility of I_2 from dissolver	>99%
10. Halide inventory from burnup	
$^{127}I + ^{129}I$	470 kg/y
^{81}Br	27 kg/y
^{81}Br normalized to ^{129}I	43 kg/y
total halides as ^{129}I	513 kg/y

After regeneration of the AgZ bed, it would be placed on standby status to remove iodine from the DOG after the parallel AgZ bed is saturated with iodine. With this design, the two AgZ beds would be regenerated five times a year.

Plans for Next Quarter

A study of the effect of dew point, NO , and NO concentration on the iodine loading of 15-cm-deep beds of AgZ will be completed. A topical report covering the laboratory effort from February to October 1977 will be drafted. The process-flow diagram for AgZ regeneration and recycle will be updated. The iodine adsorbent program will be terminated.

TABLE 4

Fundamental Data from Laboratory Observations

1.	Iodine loading on AgZ	$\geq$ 100 mg I_2/g AgZ
2.	Iodine loading on PbX	$\geq$ 300 mg I_2/g PbX
3.	Dry density of AgZ	0.79 g/cm^3
4.	Dry density of PbX	0.85 g/cm^3
5.	Desorption rate of HI from AgZ at 500°C, 1 atm and 15 m/min face velocity	4.5 mg HI/min·cm^2 in pure H_2
6.	Pressure drop across AgZ at 150°C, 1 atm and 15 m/min face velocity	0.097 atm/m in air
7.	Pressure drop across AgZ at 500°C and 15 m/min face velocity	0.03 atm/m in hydrogen
8.	Pressure drop across PbX at 150°C and 11 m/min face velocity	0.02 atm/m in hydrogen

TABLE 5

Design Criteria for AgZ and PbX Beds

		face velocity (m/min)	diam (m)	length (m)	volume (m^3)	weight (Mg)	iodine loading (kg)
1.	AgZ primary	15	0.63	2.1	0.65	0.51	51
2.	AgZ backup	19	0.63	0.5	0.15	0.12	12[b]
3.	PbX storages[a]	11	0.55	3.2	0.76	0.64	192
4.	PbX backup	12	0.55	0.8	0.19	0.16	48[b]

---

[a] PbX storage bed consists of four self-contained cartridges designed to fit in 0.2m^3 (55 gal) drums. Number of cartridges needed per/yr = 10.6

[b] During normal operation the backup beds would not be loaded with iodine.

III. WASTE MANAGEMENT[a]

(B. E. Paige)

Liquid waste from spent nuclear fuels is concentrated to increase storage capacity and, thereby, reduce the cost of interim storage of the liquid waste. Nitric acid waste is produced from the tributyl phosphate extraction step during the reprocessing of either defense fuel or from several alternative fuel cycles currently being considered for power reactor fuel. In fuel reprocessing, liquid waste will generally be concentrated and placed in interim storage tanks as a nitric acid solution because neutralization increases the volume of waste and interferes with some solidification processes. The primary purpose of the current waste evaporation and storage project is to study factors which affect the rate of heat transfer as well as the service life of equipment in nitric acid waste solutions. Other waste solutions will be studied as they are identified in future reprocessing studies.

Factors being investigated include formation of solids, fouling of heat transfer surfaces, and the behavior of off-gas. These factors are particularly important in liquid waste generated from power reactors because they contain high concentrations of fission products resulting from the high burn-up attained prior to discharge of the spent fuel. Also, cladding is removed prior to fuel dissolution, thus eliminating dissolved metal salts which dilute the fission products in some liquid wastes.

The behavior of materials of construction and the monitoring of corrosion in process equipment is also being investigated. A literature review of nitric acid corrosion[b] showed that very little information is available, even though failure of waste evaporators, especially reboiler tubes, has been a continual problem in nuclear fuel reprocessing. In current studies, particular attention is given to the investigation of the behavior of materials under process conditions.

Three types of simulated high level liquid waste (HLLW) solutions, which were patterned after HLLW solutions used in other waste studies[c], were used initially for the current program. Data from these solutions were compared to data from wastes simulating more recent estimates of acidic HLLW compositions[d]. Solids formation, physical properties, and corrosion behavior were found to be far more dependent on nitric acid concentration, total solids, and dissolved corrosion product concentration

---

[a] Part of the program Alternative Fuel Cycle Technology administered by Savannah River Operations and Savannah River Laboratory.

[b] M. W. Wilding and B. E. Paige, Survey on Corrosion of Metals and Alloys in Solutions Containing Nitric Acid, ICP 1107 (December 1976).

[c] LWR Fuel Reprocessing and Recycle Progress Report for April 1 - June 30, 1976, ICP-1101 (November 1976).

[d] LWR Fuel Reprocessing and Recycle Progress Report for January 1 - March 31, 1977, ICP-1116 (April 1977).

than on variations in the fuel or the process being simulated. The exception, however, is that high concentrations of iron, which can result from dissolution of fuel dissolver baskets, affect both corrosion and solids formation.

Current studies are continuing with a typical simulated HLLW expected from a tributyl phosphate extraction process. The HLLW contains gadolinium as nuclear poison and natural uranium as the actinides (uranium, thorium, and plutonium). Low levels of phosphate, which represent effective operation of solvent clean-up equipment and estimated levels of corrosion products from process equipment are added.

1.0 Evaporation

The evaporation studies for this quarter were performed in the small-scale thermosiphon evaporator unit. The unit was operated to identify operating problems with solutions containing solids, to investigate evaporation of HLLW from a tributyl phosphate extraction process, and to evaluate corrosion of a Type 304L stainless steel reboiler tube specimen. The corrosion results are reported in Section 3.0.

Figures 2 and 3 show the evaporator and auxiliary equipment which are located inside a 3-metre (10-feet) ventilated enclosure to permit use of actinides in waste solutions. The bottom view shows the reboiler steam section, the preheater steam section, the recycle section, and the product and condensate collection system. The top view shows the feed tank, the vapor head, the demister section, and the condenser. A sketch of the small-scale evaporator was published previously[a].

The evaporator was operated with simulated HLLW and with nitric acid. Two levels of evaporation were selected for investigation. According to earlier laboratory evaporation of HLLW, 340 L/MTU (90 gal/MTU) represents the practical limit of concentration from the standpoint of total solids content. A concentration of 1380 L/MTU (365 gal/MTU) is estimated to be the concentration limit with respect to heat removal in storage tanks where in-tank cooling coils are the primary source for heat removal. Based on these limits, the runs were made at three operating conditions as follows:

(1) The evaporation of 20 litres of solution from 4900 L/MTU at 2.5 $\underline{M}$ nitric acid to 1380 L/MTU at 7.5 $\underline{M}$ nitric acid in 48 h.

(2) The evaporation of 20 litres of reconstituted solutions from Evaporation 1 from 4900 L/MTU at 2.5 $\underline{M}$ nitric acid to 340 L/MTU at 7 to 9 $\underline{M}$ nitric acid in 62 h.

(3) The recirculation of the solution from Evaporation 2 at 340 L/MTU for an additional 48 h while recycling all condensate.

---

[a] LWR Fuel Reprocessing and Recycle Progress Report for July 1 - September 30, 1976, ICP-1108 (December 1976).

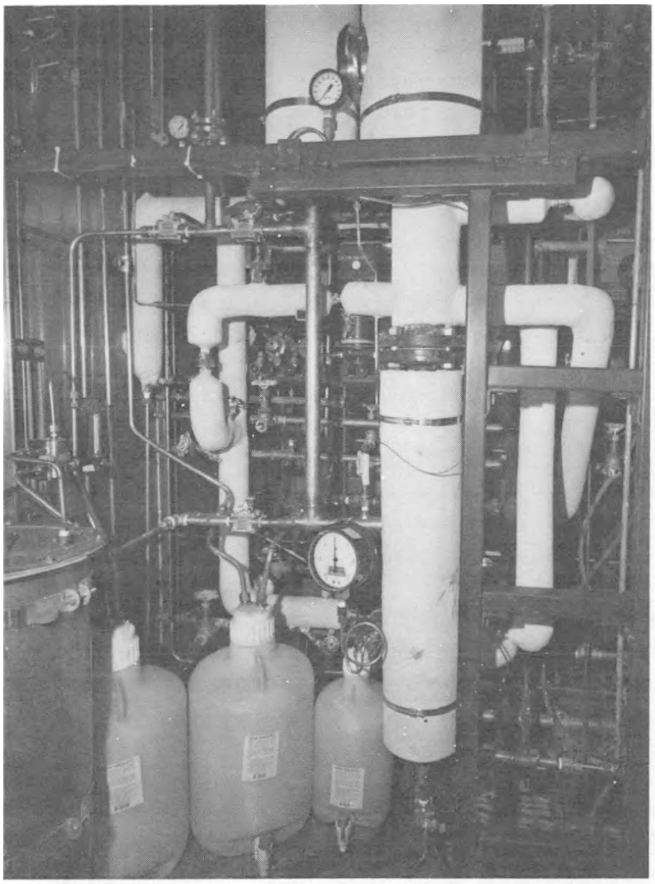

Figure 2. Lower Portion Thermosiphon Evaporator

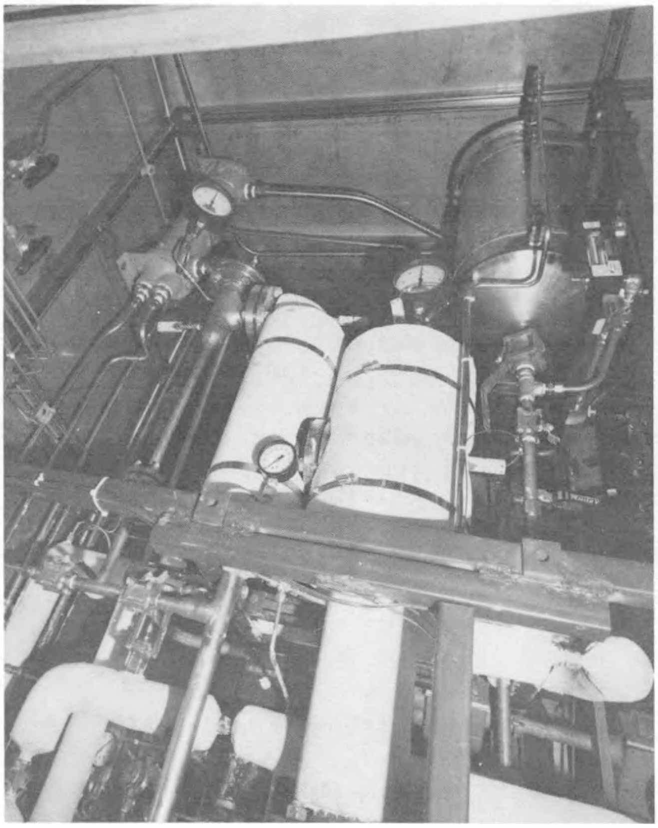

Figure 3. Upper Portion Thermosiphon Evaporator

A complete set of runs was first made with nitric acid to establish a baseline for the Type 304L stainless steel reboiler tube material. Evaporations were performed at the same conditions using simulated HLLW. The HLLW feed contained 6 g/L total fission products which represent extraction raffinate at 4900 L/MTU from fuel irradiated to 33,000 MWd/MTU and cooled for 150 days. The feed HLLW also contained 2 g/L uranium, 7 g/L gadolinium, 0.34 g/L phosphate and 0.01 g/L dissolved corrosion products.

The simulated HLLW solutions were prepared by combining stock solutions in an appropriate manner as to approximate the introduction of the components into an actual process solution. The advantages of using a series of stock solutions to prepare simulated HLLW are (1) the flexibility to rapidly prepare solutions of various concentrations of selected components, and (2) less undissolved solids in the simulated waste solution than when all reagents are added at once to a single vessel for dissolution[a]. Solution concentrations used to charge the evaporator were at the expected level of the evaporator product and were boiled during preparation to insure steady state conditions at the start of the run.

1.1 Operating Characteristics of Evaporator (G. R. Villemez, C. B. Millet)

The fast settling rate of the undissolved solids in the concentrated HLLW solution caused plugging during the operation of the thermosiphon evaporator. Most of the plugging problems were experienced at the higher concentrated solution level of 340 L/MTU as compared to a concentration level of 1380 L/MTU. Previously, laboratory evaporations have shown that there were 12% undissolved solids in HLLW solutions concentrated to 340 L/MTU. These solids settled within 10 minutes, but were easily suspended with gentle agitation.

In the thermosiphon evaporator, the feed line became plugged due to settled solids which collected below the recycle line in the area of the preheater. Air pressure applied to the feed line dislodged the solids easily. Unstable operating conditions occurred whenever the evaporator became plugged; an increase in the reboiler temperature and a decrease in HLLW recirculation resulted. The feed line is currently being connected directly below the reboiler tube to eliminate the pocket resulting from the pre-heater installation; this should minimize the plugging problem for future operations. An automatic control valve in the feed line will also be installed with a control signal from the evaporator-heat pressure to assist in maintaining a stable operating liquid level.

The thermosiphon evaporator operated very well in a total recycle mode for 48 hours with HLLW at the 340 L/MTU level.

1.2 Heat Transfer of Evaporator (G. R. Villemez, C. B. Millet)

The rate of heat transfer, q, is expressed as the product of three factors: the over-all heat transfer coefficient (U), the area of the heat

---

[a] LWR Fuel Reprocessing and Recycle Progress Report for April 1 - June 30, 1976, ICP-1101 (November 1976).

transfer surface (A), and the temperature difference (ΔT). The relationship is

$$q = U \cdot A \cdot \Delta T.$$

The area is based on the inside diameter of the 1-inch reboiler tube. The reboiler tube exposed to the condensing steam was 30 cm (12-inches) in length; an additional 15 cm (6 inches) of the reboiler tube were exposed to the condensate. The apparent temperature difference was calculated from the condensing steam temperature and the measured saturated vapor temperature above the boiling liquid. The feed solution was preheated by steam to the temperature of the recirculated solution. The solution temperature was near the boiling point at the feed end of the reboiler section. This resulted in utilizing the entire length of the reboiler tube as a corrosion specimen.

The maximum allowable steam temperature in a waste evaporator is 130°C due to the explosion hazard of tributyl phosphate and nitric acid in actual process conditions. Within this temperature limit, the small-scale evaporator can be operated at a vapor velocity of 0.3 to 1.22 m/s (1 to 4 ft/s) using the steam control.

No data are available for the decomposition of nitric acid during evaporation.

The rate of heat transfer, q, was calculated as the product of the latent heat of evaporation of water at the saturated vapor temperature and the vapor rate at the atmospheric pressure of 84.7 kPa (12.3 psi) at 1585 metres (5200 ft) elevation. The calculated heat transfer rates should be within 10% of the actual value.

1.21 Rate

The apparent over-all heat transfer coefficient for current runs was calculated from operating data taken during steady-state conditions. These preliminary data are shown in Figure 4 for nitric acid and HLLW during evaporation from 4900 L/MTU containing 2.5 M nitric acid.

The over-all heat transfer coefficient increased as the vapor rate increased. The vapor condensate composition was in the range of 2 to 3 M nitric acid. A vapor rate of 300 g/h is equivalent to 0.3 m/s (1 ft/s) vapor velocity in the reboiler tubes assuming the vapor volume of water. The over-all heat transfer coefficients for the HLLW solutions were 70 to 80% of the base line nitric acid values. The coefficients varied from 760 to 2080 $W/m^2 \cdot K$ (134 to 367 $BTU/h \cdot ft^2 \cdot °F$) depending on the vapor velocities which varied from 0.3 to 1.22 m/s (1 to 4 ft/s). Since the heat transfer coefficients were similar for nitric acid and HLLW at lower solids content (1380 L/MTU and 7.5 M nitric acid), the lower heat transfer coefficients for HLLW solutions at the 340 L/MTU level may be due to the scale formed from the HLLW solution on the reboiler tube as well as to changes in the physical properties of the solution.

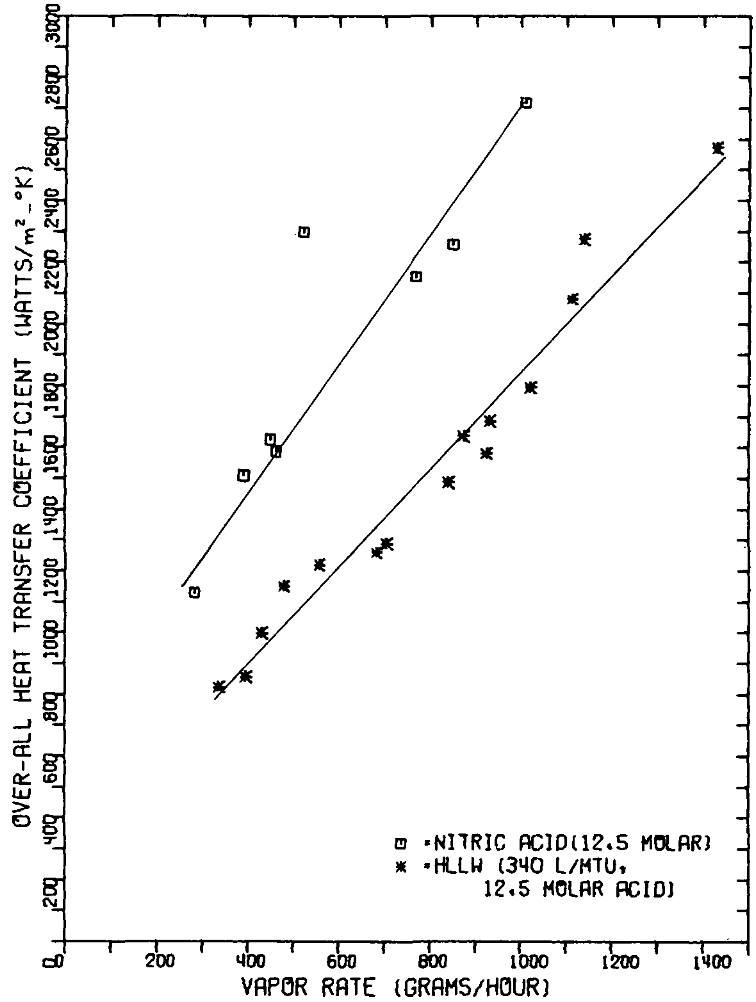

Figure 4. Heat Transfer Data for Initial Evaporator Runs

1.22 Scaling and Fouling

Scale was formed in the reboiler tube section during the evaporation of the simulated HLLW waste solution. Scale results in a fouling factor for the overall heat transfer coefficient during the evaporation process. Scale deposited on the feed end of the reboiler tube is shown in Figure 5. The scale deposit was thicker, as shown in Figure 6, in the top of the reboiler tube which was exposed to the steam and hence, the maximum temperature. This figure shows that scale did not form uniformly on the tube sheet.

1.23 Nature of Scale

X-ray diffraction patterns indicate that a major component of the scale consists of the hydrated zirconium-molybdenum compound which is also the major component in the precipitates from laboratory evaporations

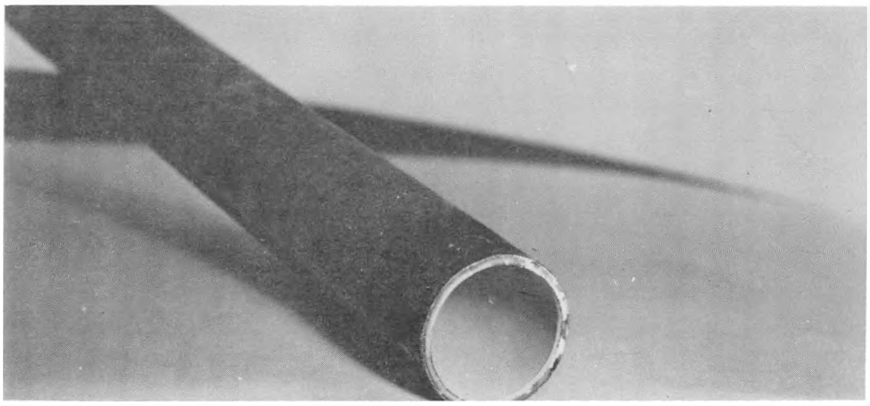

TYPE 304L S.S. REBOILER TUBE EXPOSED
TO LWR WASTE SOLUTION - 1

Figure 5. Scale on Feed End of Reboiler Tube

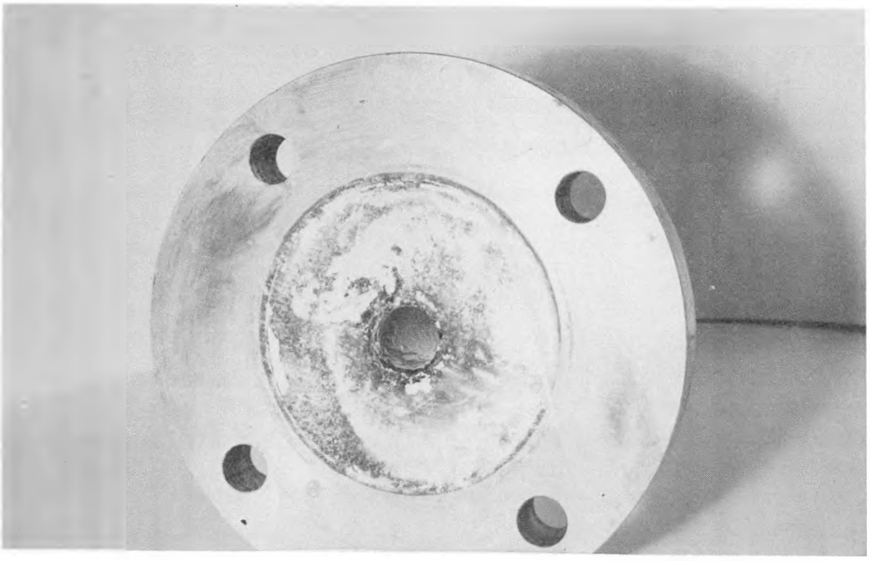

TYPE 304L S.S. REBOILER TUBE EXPOSED
TO LWR WASTE SOLUTION - 1

Figure 6. Scale on Tube Sheet and Top End of Reboiler Tube

of HLLW. The X-ray pattern for the remainder of the material corresponds to the pattern for $Fe(UO_2)_2(PO_4)_2 \cdot nH_2O$. The latter compound was identified in scale deposits on the glass laboratory evaporator but not in the undissolved solids of the evaporated slurries. Examination of the scale by scanning electron microscope (SEM) shows that the solids are not definite crystals as have been precipitated from HLLW slurries evaporated in the glass laboratory evaporator. Additional examinations will be made to determine if similar scale has formed in other parts of the evaporator, and methods of descaling will be investigated.

2.0 Waste Storage

Studies are currently in progress to determine the behavior of HLLW solutions and slurries during interim storage. This information will provide the basis for improved and economical design of future liquid waste storage tanks. The data obtained will also permit more efficient and safer operation of existing liquid waste storage tanks.

During this quarter, the major effort has been expended in developing laboratory equipment and techniques which can adequately provide the desired information and data. In addition, long-term characterizations of simulated HLLW solutions are continuing.

2.1 Laboratory Storage Tank (P. A. Anderson)

A laboratory tank has been constructed for storage studies using simulated HLLW. The purposes are: 1) to develop techniques for laboratory waste storage studies, 2) to modify and improve the design of future experimental equipment, and 3) to obtain preliminary data on the behavior of stored HLLW slurries with respect to mixing, stability, heat transfer, scaling, and corrosion of materials exposed to HLLW.

2.11 Design of Equipment

The present experimental equipment, shown in Figure 7, consists of a 13.6 L(3.6 gallon) glass tank with a transparent plastic lid and a high efficiency condensor. The tank is enclosed in a transparent plastic cubicle which is heated to the same temperature as the stored solution to prevent heat loss from the solution to the air. The cubicle air temperature is thermostatically controlled by a 110-V, 660-W resistance heater and a small circulating fan.

Fission product decay heat is simulated in the solution by a 110-V, 600-W immersed resistance heating coil. The heating coil can be either thermostatically controlled or operated to deliver measured amounts of heat from 0 to 680 W (2300 Btu/h) by a calibrated rheostat. The resistance of the heater was determined to be constant at 23.0 ohms over the temperature range of 40 to 60°C.

The Type 304L stainless steel cooling coil has an outside diameter of 0.63 cm (0.25 in.) and an inside diameter of 0.524 cm (0.206 in.). The total cooling coil surface area is 245 cm^2 (0.263 ft^2). The cooling water flow is regulated by a valved rotometer with an operating range of

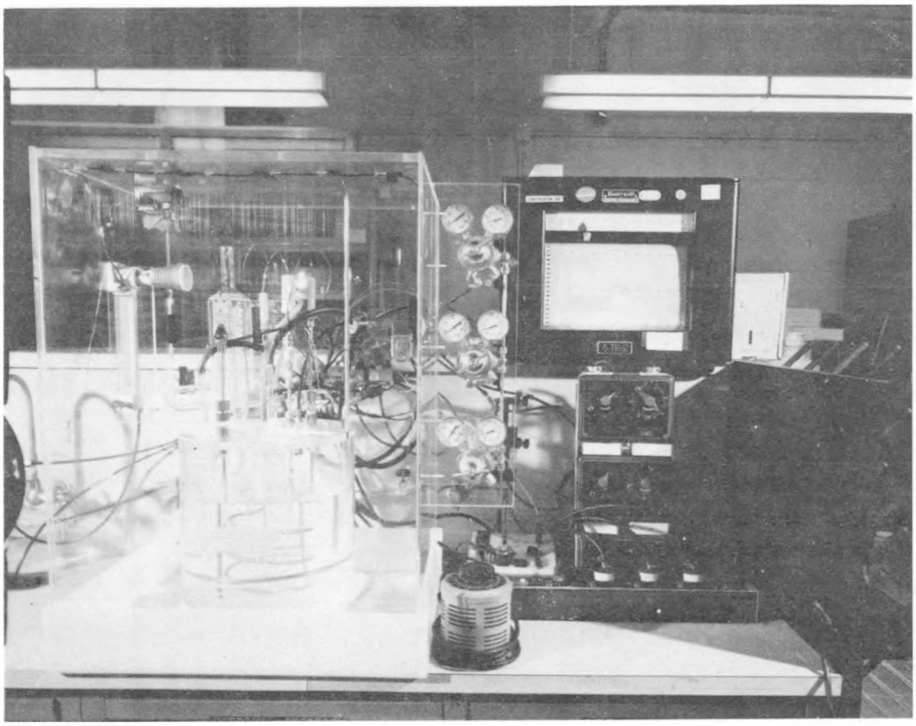

Figure 7. Laboratory Storage Tank

0 to 8 cm^3/s. Accurate flowrate measurements are obtained by weighing timed increments of effluent cooling water. All inflowing water lines and the condenser are covered with foam insulation to minimize heat transfer to the cooling water from the heated air inside the cubicle.

Thermocouples are in the following locations: 1) in the inflowing and outflowing cooling water lines at the surface of the stored solution, 2) in the stored solution at points 5 cm from the top and 5 cm from the bottom of the tank, and 3) in the transparent plastic cubicle both above and beside the tank. Temperatures are recorded at one minute intervals.

Mixing of the stored solution is obtained with two glass airlift circulators which are designed for continuous or intermittent operation. Two glass ballast tank agitators, powered by compressed air, are primarily designed to suspend undissolved solids which settle to the bottom of the tank; however, they also contribute to the mixing of the solution. The frequency of expelling solution from the ballast tanks is controlled by cyclic timers and three-way solenoid valves. Air which is displaced from the ballast tanks is vented into the storage tank.

The present experimental equipment is designed to simulate a typical large 1,100,000 litre (300,000 gallon) storage tank using a scale down factor of approximately 10^5. Table 6 shows the design criteria which were selected for the laboratory storage tank. These criteria are based

TABLE 6

Design Criteria of Laboratory Storage Tank[a]

Discharge velocity of ballast tank nozzle		18 m/s (59 ft/s)
Ratio of total volume of ballast tanks to volume of solution		4.8×10^{-2}
Cooling coil water:	Flowrate per liter of stored solution	2.06×10^{-4} L/s
	Inflowing temperature (T_i)	35°C
	Outflowing temperature (T_o)	46°C
	Temperature of stored solution (T_s)	60°C
Ratio of cooling coil surface to solution volume		$18\ cm^2/L$ ($.072\ ft^2/gal$)

---

[a] Based upon the design of HLLW storage tanks described in Final Safety Analysis Report, Barnwell Nuclear Fuel Plant Separation Facility, Amendment No. 1, April 1, 1974, Sections 8 and 9.

upon the newest liquid waste storage tanks in the United States. The waste tank design is suitable for high-level heat generating wastes from different types of reactors. It is similar in design but more advanced than the stainless steel tanks used to successfully store acidic waste containing nitric acid and fluoride at ICPP.

Numerous improvements were made in the laboratory tank and equipment during the early operation with water as the stored solution. A more sensitive electronic thermostat was installed to maintain the cubicle temperature within one degree Celsius. Fluctuations in the cooling water temperature were eliminated with increased insulation and by installing a constant temperature bath to regulate the temperature of the inflowing cooling water. A mechanical stirrer was installed to provide supplementary mixing when the airlift circulators are not operating. Plastic filings were put in the solution to aid visual observation of physical mixing during the equipment testing with water.

2.12 Heat Transfer

In order to verify the operating characteristics of the laboratory storage tank, heat transfer measurements were made using water at 60°C (140°F) and 49°C (120°F) with the heat source thermostatically controlled with known amounts of heat input. Heat transfer coefficients for the tank are shown in Figure 8 for various flowrates. The data points marked by asterisks were obtained at operating conditions which correspond to

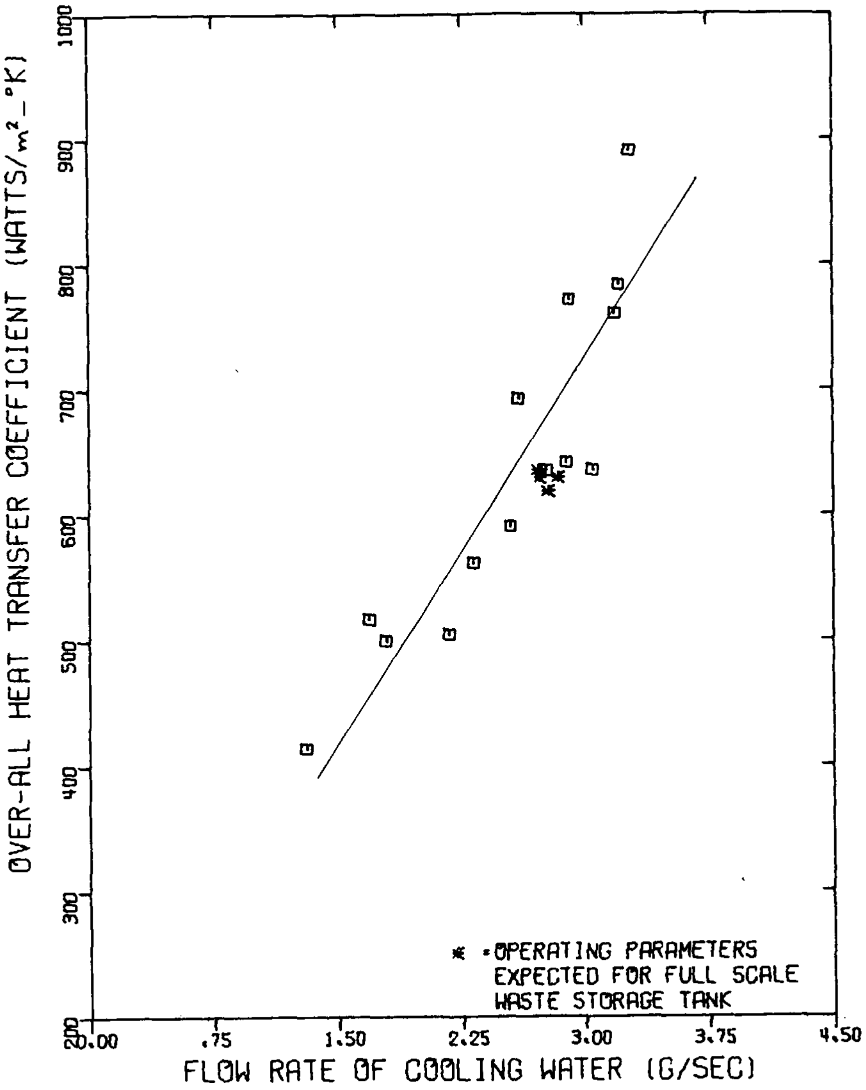

Figure 8. Heat Transfer Coefficients Obtained for Water in Laboratory Storage Tank

those expected in a typical large storage tank with respect to the flowrate, inflowing temperature, and outflowing temperatures of the cooling water. The cooling coil water flow is entirely in the laminar flow range because turbulent flow could not be attained in the small tank at the selected design criteria. A Reynolds number of approximately 1000 is obtained at a nominal flowrate of 2.8 g/s.

2.13 Heat Balance

Heat balance measurements were also made for the laboratory storage tank. The rate of heat input was controlled by a calibrated rheostat on the solution heating coil. The rate of heat removal was determined from the increase in temperature of weighed quantities of cooling water. The solution was continuously mixed by both airlift circulators and ballast tank agitators.

As shown in Table 7, an average of 20 percent of the input heat is lost from the solution by means other than the cooling coil. Part of this loss may be attributed to evaporation into air discharged through the airlift circulators. Estimates made on the basis of the volume of air discharged indicate that airlift circulators emitting dry air at a rate of 23 cm /s (.049 ft /min) should remove approximately 13 W. However, comparison of the rate of solution temperature change with the airlift circulators operating to the rate of change with them turned off, indicates that heat is actually removed at approximately three times that rate. Other possible sources of heat loss which will be investigated include the evaporation of the solution into the air vented from the ballast tanks and the cooled condensate returning from the condenser.

TABLE 7

Heat Balance in Laboratory Storage Tank

Heat Input (H_i) to Stored Solution, W	Heat Removed (H_o) via Cooling Coil, W	Percent of Heat Removed via Cooling Coil
185	122	66
185	120	65
185	121	65
202	173	86
302	326	108
315	250	79
331	323	98
372	258	69
440	348	79
501	401	80
645	530	82
645	538	83
680	533	78
		Average = 80

2.2 Storage of Evaporated HLLW (P. A. Anderson)

Long-term storage studies of evaporated simulated HLLW slurries, at constant temperature and without agitation, are continuing. The slurries have been monitored at intervals of one to two months for stability with respect to quantities of undissolved solids. The data obtained from

18 samples, some stored up to 11 months, were analyzed statistically. The relationship between quantity of undissolved solids and length of time stored was significant at the 0.1 confidence level in 2 of the 18 samples, but duplicates of these samples did not show significant changes. It is concluded that the quantity of undissolved solids in evaporated HLLW slurries has not changed significantly during interim storage for up to one year.

3.0 Materials and Corrosion

Materials and corrosion studies are being conducted in the laboratory and in small-scale equipment to establish the effect of waste composition and components on materials of construction and to investigate new materials for evaporators, waste tanks, and auxiliary equipment. In addition, methods for monitoring corrosion of waste tanks during interim storage of liquid waste are being investigated.

3.1 Monitoring of Storage Tanks (P. A. Anderson)

Microscopic examination of three electronic corrosion monitoring probes yielded no evidence of pitting or cracking in Type 304L stainless steel after four months of exposure at 60°C to simulated HLLW-0 (contains minimal process additives), HLLW-Fe (contains high iron), and HLLW-UP (contains high uranium and phosphate). There was visual evidence of general surface attack and very small amounts of scaling of solids on probe surfaces.

The evaluation of the Type 304L stainless steel monitoring probes is continuing with new HLLW slurries containing high levels of nitric acid and uranium as a simulant for total actinides. The present solutions contain palladium and rhodium, which were previously substituted, and gadolinium and ruthenium, which were previously omitted. A monitoring probe has also been installed in the laboratory storage tank.

3.2 Reboiler Tube Evaluation (G. R. Villemez, C. B. Millet)

A Type 304L stainless steel welded reboiler tube was evaluated for corrosion rates during the operation of the thermosiphon evaporator with nitric acid and HLLW expected from a tributyl phosphate extraction process. Only general attack was visible in the reboiler tube after the scale was removed. The corrosion rate of the reboiler tube during 500 hours of evaporator service was 517 μm/yr (20.4 mils/yr) according to calculations from the weight loss and the total area of the reboiler tube. Based on the measured change of the inside diameter of the tube at the feed end, the corrosion rate was 523 μm/yr (20.6 mils/yr). The excellent agreement between these two values showed that the attack was uniform over the entire area of the reboiler tube.

Some weld decay occurred on the Type 304L stainless steel plate near the weld in the heat affected zone. Crevice corrosion can be seen in the outer area of the plate near the gasket location while general corrosion occurred on the face of the plate as shown in Figure 9.

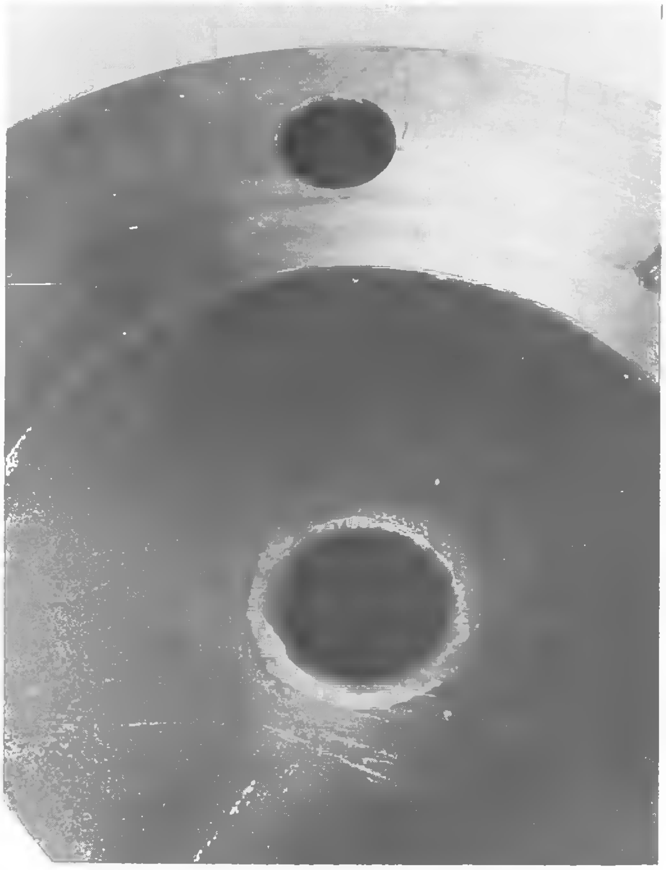

Figure 9. Crevice Corrosion and Weld Decay on Type 304L Stainless Steel Tube Sheet (Exposed 500 h to nitric acid and HLLW at boiling)

The evaporated solutions were analyzed for iron content to determine the quantity of corrosion products dissolved in each of the evaporator runs. Using the calculated exposed area, an average corrosion rate for the entire evaporator was calculated for the evaporated solution in each run. The average corrosion rate for all of the runs was 243 μm/yr (9.6 mils/yr); this indicates the reboiler tube experienced nearly twice the corrosion attack as the rest of the stainless steel evaporator surface.

The buildup of the corrosion product level in the solutions will limit the time that solutions can be used for evaporator tests because the corrosion rate of Type 304L stainless steel accelerates as the corrosion product level increases above 1 g/l[a]. In the thermosiphon evaporator,

---

[a] LWR Fuel Reprocessing and Recycle Progress Report for January - March 31, 1977, ICP-1116 (April, 1977).

the corrosion product level increased faster in the HLLW solutions during evaporation than in the nitric acid solution, and the rate of increase depended on the acid concentration. During 68 hours of continuous operation, the corrosion products concentration increased from 0.2 g/L to 5.2 g/L in HLLW. However, the increase was only from 5.2 g/L to 6.2 g/L in 50 hours of operation in a recycle mode with the vapor condensate returning to the reboiler. This may have been due either to the formation of the scale on the evaporator surface or to the precipitation of the corrosion products.

These corrosion data are considered preliminary since this was the initial operation of the evaporator and some plugging occurred. More information on the effects of the stainless steel evaporator unit will be obtained using a titanium reboiler tube.

Plans for Next Quarter

The small-scale thermosiphon evaporator will be modified and improved to reduce plugging during operation with simulated HLLW solutions which are highly concentrated and contain considerable amounts of undissolved solid. The evaporator will be operated with a titanium reboiler tube specimen using nitric acid as a base line and several levels of HLLW as was done with the Type 304L stainless steel specimen. A comparison of heat transfer characteristics, scaling, and corrosion will be made between the two materials.

Laboratory corrosion tests will be performed to determine the effect of technetium, ruthenium, and cerium; the latter is the major component of commercial rare earth mixtures. Long term stability tests and evaluation of corrosion monitoring probes will continue.

The laboratory storage tank will be operated with nitric acid and simulated HLLW containing large amounts of undissolved solids to determine heat transfer and heat balance characteristics and to investigate the effect of scaling and mixing. The rate of loss of HNO from the high efficiency condenser will be investigated.

INTERNAL DISTRIBUTION

1. C. B. Amberson
2. F. H. Anderson
3. P. A. Anderson
4. J. C. Bishop
5. R. A. Brown
6. B. R. Dickey
7. W. A. Freeby
8. D. A. Knecht
9. H. Lawroski
10. L. C. Lewis
11. F. L. McMillan
12. C. B. Millet
13. B. C. Musgrave
14. B. E. Paige
15. K. L. Rohde
16. T. R. Thomas
17. G. R Villemez
18. B. R. Wheeler
19. M. W. Wilding
20. C. M. Slansky

A. T. Morphew (3)
Classification & Technical Information Officer
Idaho Operations Office, ERDA

Chicago Patent Group, ERDA
9800 South Cass Avenue
Argonne, IL 60439

H. P. Pearson, Supervisor
Technical Information
EG&G

INEL Technical Library (10)

EXTERNAL DISTRIBUTION

36. R. C. Adkins, Technical Representative, NUSAC, 777 Leesburg Pike, Falls Church, VA 22043
37. EG&G Idaho, Incorporated, P.O. Box 1625, Idaho Falls, ID 83401
38. H. M. Agnew, Director, Los Alamos Scientific Laboratory, P. O. Box 1663, Los Alamos, NM 87545
39. T. W. Ambrose, Director, Pacific Northwest Laboratory, P. O. Box 999, Richland WA 99352
40. C. K. Anderson, Combustion Engineering Nuclear Power Division, 1000 Prospect Hill Road, Windsor, CT 06095.
41. Argonne National Laboratory, P. O. Box 2528, Idaho Falls, ID 83401
42. Argonne National Laboratory, 9700 South Cass Avenue, Argonne, IL 60439.
43. J. F. Bader, Manager, Plutonium Recycle Fuel Programs, Westinghouse Electric Corporation, Box 355, Pittsburgh, PA 15230
44. G. W. Cunningham, Division of Nuclear Fuel Cycle and Production, U. S. Energy R&D Administration, Washington, DC 20545
45. Battelle-Columbus Laboratories, 505 King Avenue, Columbus, OH 43201
46. M. Binstock, Kerr-McGee Nuclear Corporation, Kerr-McGee Building, Oklahoma City, OK 73102

47. K. Bowlman, General Electric Company, 175 Curtner Avenue, San Jose, CA 95125
48. R. G. Bradley, Division of Nuclear Fuel Cycle and Production, U.S. Energy R&D Administration, Washington, DC 20545
49. M. G. Britton, Manager Technical Liaison, Corning Glass Works, Corning, NY 14830
50. J. Carp, Director for Energy Policy, Edison Electric, 90 Park Avenue, New York, NY 10016
51. W. T. Cave, Director, Monsanto Research Corporation, Mound Laboratory, P. O. Box 32, Miamisburg, OH 45332
52. B. H. Cherry, Manager of Fuel Resources, GPU Services Corporation, 260 Cherry Hill Road, Parsippany, NJ 07054
53. G. R. Corey, Vice Chairman, Commonwealth Edison Company, P. O. Box 767, Chicago, IL 60690
54. R. G. Cross, DBM Corporation, 1920 Alpine Avenue, Vienna, VA 22180
55. R. Cunningham, Nuclear Materials Safety and Safeguards, Nuclear Regulatory Commission, Washington, DC 20555
56. R. L. Dickeman, President, Exxon Nuclear Company, Inc., 777 106th Avenue, NE, Bellevue, WA 98004
57. Electric Power Research Institute, P. O. Box 10055, Palo Alto, CA 94303
58. R. Fullwood, Science Applications, Inc., 2680 Hanover Street, Palo Alto, CA 94303
59. R. L. Grant, Director of Nuclear Projects, Boeing Engineering and Construction Division, P. O. Box 3707, Seattle, WA 98124
60. Hanford Engineering Development Laboratory, Associate Lab Director, P. O. Box 1970, Richland, WA 99352
61. T. B. Hindman, Jr., Director, Fuel Cycle Project Office, U. S. Energy R&D Administration, Savannah River Operations Office, P. O. Box A, Aiken, SC 29801
62. A. H. Hines, Jr., President, Florida Power Corporation, P. O. Box 14042, St. Petersburg, FL 33733
63. C. A. Hirenda, Director of Marketing, Proposal Management, Inc., 121 N. Orionna Street, Philadelpha, PA 19106
64. P. Hogroian, Division of Nuclear Fuel Cycle and Production, U..S. Energy R&D Administration, Washington, DC 20545
65. R. Hoskins, Tennessee Valley Authority, 217 Electric Power Board Building, Chattanooga, TN 37401
66. C. H. Ice, Director, Savannah River Laboratory, E. I. duPont deNemours and Company, Aiken, SC 29801
67. R. H. Ihde, Manager, Contracts and Marketing, Babcock and Wilcox, P. O. Box 1260, Lynchburg, VA 24505
68. W. Johnson, Vice-President, Yankee Atomic Electric Company, 20 Turnpike Road, Westboro, MA 01581
69. W. A. Kalk, Manager, Nuclear Power Systems, Holmes and Narver, Inc., 400 East Orangethorne Avenue, Anaheim, CA 92801
70. M. I. Kaparstek, Manager of Proposals, Burns and Roe, Industrial Services Corporation, P. O. Box 663, Paramus, NJ 07652
71. K. Killingstad, Cont. Services, Battelle-Human Affairs Research Centers, 4000 N. E. 41st Street, Seattle, WA 98105
72. H. Kouts, Nuclear Regulatory Commission, Washington, DC 20555
73. C. Kuhlman, Division of Nuclear Cycle and Production, U. S. Energy R&D Administration, Washington, DC 20545

74. J. A. Kyger, Associate Director, Argonne National Laboratory, 9700 South Cass Avenue, Argonne, IL 60439
75. F. W. Lewis, President, Middle South Utilities, Inc., Box 61005, New Orleans, LA 70161
76. W. H. Lewis, Nuclear Fuel Services, 6000 Executive Blvd., Rockville, MD 20952
77. J. L. Liverman, Division of Biomedical and Environmental Research, U. S. Energy R&D Administration, Washington, DC 20545
78. H. E. Lyon, Division of Safeguards and Security, U. S. Energy R&D Administration, Washington, DC 20545
79. L. W. Nelms, Chief, Research Branch, Research and Technical Division, Todd Company, P. O. Box 1600, Galveston, TX 77550
80. R. D. Oldenkamp, Rockwell International, Atomics International Division, 8900 De Soto Avenue, Canoga Park, CA 91304
81. G. B. Pleat, Division of Nuclear Fuel Cycle and Production, U. S. Energy R&D Administration, Washington, DC 20545
82. Herman Postma, Director, Oak Ridge National Laboratory, P. O. Box X, Oak Ridge, TN 37830
83. G. K. Rhode, Vice-President-Engineer, Niagara Mohawk Power Corp., 300 Erie Boulevard, West, Syracuse, NY 13202
84. L. M. Richards, Nuclear Commercial Development Coordinator, Atlantic Richfield Company, Box 2679 - TA, Los Angeles, CA 90071
85. R. W. Roberts, Assistant Administrator for Nuclear Energy, U. S. Energy R&D Administration, Washington, DC 20545
86. R. C. Baxter, President, Allied-General Nuclear Services, P. O. Box 847, Barnwell, SC 29812
87. J. Shefcik, General Atomic Company, P. O. Box 81608, San Diego, CA 92138
88. N. F. Seivering, Jr., Assistant Administrator for International Affairs, U. S. Energy R&D Administration, Washington, DC 20545
89. L. E. Smith, Manager-Fuel, Carolina Power and Light Company, P. O. Box 1551, Raleigh, NC 27602
90. D. Spurgeon, Division of Nuclear Fuel Cycle and Production, U. S. Energy R&D Administration, Washington, DC 20545
91. A. Squire, Director, Hanford Engineering Development Laboratory, P. O. Box 1970, Richland, WA 99352
92. C. Stephens, Virginia Electric Power Company, Nuclear Fuel Service Department, 512 Franklin Building, P. O. Box 26666, Richmond, VA 32361.
93. N. Stetson, Manager, U. S. Energy R&D Administration, Savannah River Operations Office, P. O. Box A, Aiken, SC 29810
94. S. Stroller, Western Reprocessors, The S. M. Stoller Corporation, 1250 Broadway, New York, NY 10001
95. K. Street, Associate Director, Lawrence Radiation Laboratory, P. O. Box 808, Livermore, CA 94550
96. G. Stukenbroeker, N. Industries, P. O. Box 928, Barnwell, SC 29812
97. J. D. Tokerud, Vice-President, Aerojet Energy Conversion Company, 1120 Connecticut Avenue, NW, Suite 1050, Washington, DC 20035
98. Dr. Uhrig, Florida Power and Light Company, P. O. Box 013100, Miami FL 33101
99. E. J. Wahlquist, Deputy Assistant Director for Terrestrial Programs, U. S. Energy R&D Administration, Washington, DC 20545
100. W. J. Wilcox, Technical Director, ARGDP, Oak Ridge, TN 27802

101. A. K. Williams, Director, Nuclear Technology Division, Allied-General Nuclear Services, P. O. Box 847, Barnwell, SC 29812
102. U. S. Energy Research & Development Administration, Chicago Operations Office, Contracts Division, 9800 South Cass Avenue, Argonne, IL 60439
103. U. S. Energy R&D Administration, Division of RDD, Energy Systems Analysis, Washington, DC 20545
104. U. S. Energy R&D Administration, Division of RDD, Engineering and Technology, Washington, DC 20545
105. U. S. Energy R&D Administration, Division of RDD, LMFBR Programs, Washington, DC 20545
106. U. S. Energy R&D Administration, Division of RDD, Reactor Safety, Washington, DC 20545
107. U. S. Energy R&D Administration, Library, Washington, DC 20545
108. U. S. Energy R&D Administration, Oak Ridge Operations Office, Manager, P. O. Box E, Oak Ridge, TN 37830
109. U. S. Energy R&D Administration, Oak Ridge Operations Office, Reactor Division, P. O. Box E, Oak Ridge, TN 37830
110. U. S. Energy R&D Administration, Patent Office, Washington, DC 20545
111. U. S. Energy R&D Administration, Richland Operations Office, P. O. Box 550, Richland, WA 99352
112. U. S. Energy R&D Administration, Southern California Energy Program Office, P. O. Box 1446, Canoga Park, CA 91304
113. U. S. Energy R&D Administration, Technical Information Center, Oak Ridge, TN 37820
114. U. S. Energy R&D Administration, Division of Reactor Development Demonstration, Washington, DC 20545
115. U. S. Energy R&D Administration, Idaho Operations Office, 550 Second Street, Idaho Falls, ID 83401
116. U. S. Energy R&D Administration, Nevada Operations Office, P. O. Box 14100, Las Vegas, NV 89114
117. U. S. Energy R&D Administration, San Francisco Operations Office, 1333 Broadway, Wells Fargo Building, Oakland, CA 94612